

Communication: Drift velocity of Brownian particle in a periodically tapered tube induced by a time-periodic force with zero mean: Dependence on the force period

V. Yu. Zitserman,¹ A. M. Berezhkovskii,^{2,a)} A. E. Antipov,³ and Yu. A. Makhnovskii⁴

¹Joint Institute for High Temperatures, Russian Academy of Sciences, Izhorskaya 13, Bldg. 2, Moscow 125412, Russia

²Mathematical and Statistical Computing Laboratory, Division of Computational Bioscience, Center for Information Technology, National Institutes of Health, Bethesda, Maryland 20892, USA

³Physics Department, Moscow State University, Leninskie Gory, Moscow 119992, Russia

⁴Topchiev Institute of Petrochemical Synthesis, Russian Academy of Sciences, Leninsky Prospect 29, Moscow 119991, Russia

(Received 16 August 2011; accepted 16 September 2011; published online 30 September 2011)

We study the drift of a Brownian particle in a periodically tapered tube, induced by a longitudinal time-periodic force of amplitude $|F|$ that alternates in sign every half-period. The focus is on the velocity dependence on the force period, which is usually considered not tractable analytically. For large $|F|$ we derive an analytical solution that gives the velocity as a function of the amplitude and the period of the force as well as the geometric parameters of the tube. The solution shows how the velocity decreases from its maximum value to zero as the force period decreases from infinity (adiabatic regime) to zero. Our analytical results are in excellent agreement with those obtained from 3D Brownian dynamics simulations. © 2011 American Institute of Physics. [doi:10.1063/1.3647873]

The problem of directed motion under the action of a time-periodic force, $F(t)$, with zero mean in a macroscopically homogeneous environment is one of the fundamental problems of nonequilibrium statistical mechanics. The problem has many different faces. Here we consider a particular case when a point Brownian particle moves in the environment that has a periodic microstructure with an asymmetric elementary cell. (When the cell is symmetric, there is no directed motion since there is no a preferential direction of motion.) The effective drift velocity of the directed motion is the difference between the particle displacements during positive and negative half-periods of the force, Δ_{\pm} , divided by the force period, τ . This velocity, $v = (\Delta_+ - \Delta_-)/\tau$, is a function of $F(t)$ and the properties of the environment. We consider a special case when $F(t)$ instantly switches between two values, $\pm|F|$, every half-period. In this case the velocity depends on the two parameters of the force, its amplitude $|F|$ and period τ , $v = v(|F|, \tau)$. The directed motion arises only when the force amplitude is not too small. If the amplitude is not large enough, the system operates in the linear response regime, where the displacements Δ_+ and Δ_- are equal in magnitude, and hence $v(|F|, \tau) = 0$.

The present Communication focuses on the τ -dependence of the drift velocity, which is usually considered not tractable analytically. For the first time, we provide an analytical solution for $v(|F|, \tau)$ assuming that the force amplitude is very large. The solution shows that $v(|F|, \tau)$ decreases monotonically with τ from its maximum value in the adiabatic regime ($\tau \rightarrow \infty$) to zero as $\tau \rightarrow 0$. The solution is obtained for the case when the particle moves in

a periodically tapered tube schematically shown in Fig. 1, assuming that the force acts along the tube axis. We show that the drift velocity factorizes as $v(|F|, \tau) = v_{ad}(|F|)f(\tau)$, where $v_{ad}(|F|) = v(|F|, \infty)$ is the drift velocity in the adiabatic regime and $f(\tau)$ is independent of $|F|$ and increases monotonically from zero to unity as τ increases from zero to infinity, Eq. (4). We find that $v_{ad}(|F|) \propto |F|$ at large $|F|$, and establish the relation between the ratio $v_{ad}(|F|)/|F|$ and the geometric parameters of the tube, Eq. (1). We derive a general solution for $f(\tau)$ as an infinite series of Bessel functions, Eq. (11), which is in excellent agreement with $f(\tau)$ obtained from 3D Brownian dynamics simulations over the entire range of τ (Fig. 3). We also find simple expressions for the asymptotic behaviors of $f(\tau)$, as $\tau \rightarrow \infty$ and 0, Eqs. (5) and (7), and suggest a simple approximate formula, Eq. (8), which describes the variation of $f(\tau)$ from zero to unity, as τ goes from zero to infinity.

The problem of directed motion under the action of a time-periodic force with zero mean in a spatially periodic asymmetric environment has been discussed in numerous publications, since it arises in many different contexts, ranging from biology to nanotechnology (see review articles¹ and references therein). Periodic asymmetry of the environment may be due to a periodic asymmetric energy potential, $U(x)$, $U(x + l) = U(x)$, where x is a coordinate measured along the force direction, and l is the period. Alternatively, this can be due to periodic in x variation of the geometric constraints, for example, as shown in Fig. 1. One can recast the varying tube geometry into periodic entropy potential $U_{ent}(x) = -k_B T \ln[A(x)/A_{\min}]$, where $A(x)$ is the tube cross-sectional area at a given value of x , A_{\min} is the minimum cross-sectional area, k_B is the Boltzmann constant, and T is the absolute temperature. While most publications deal with

^{a)} Author to whom correspondence should be addressed. Electronic mail: berezh@mail.nih.gov.

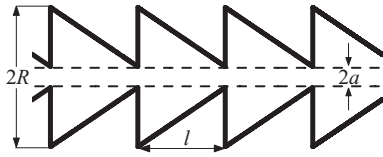


FIG. 1. Schematic representation of a periodically tapered tube. Dashed lines show the cylindrical tube connecting the openings.

the case of the periodic energy potential, there are a few recent papers in which directed motion in the presence of periodically varying geometric constraints has been studied.²⁻⁷

The directed motions induced by the time-periodic force with zero mean in periodic asymmetric energy and entropy potentials are similar on condition that the entropy potential (tube geometry) is a smoothly varying function. The reason is that the force-dependent mobility of the particle, $\mu(F)$, has a similar behavior in both cases. The mobility is a non-monotonic function of F that tends to its value in the absence of the periodic energy/entropy potential, μ_0 , as $F \rightarrow \pm\infty$, having a minimum in-between. In the case of the periodic energy potential, the asymptotic behavior, $\mu(\pm\infty) = \mu_0$, follows from the fact that, at sufficiently large F , the energy $|F|$ significantly exceeds the amplitude of the periodic potential, and the latter can be considered as a negligibly small perturbation as $F \rightarrow \pm\infty$.⁸ The situation is different in a tube of smoothly varying geometry. Here collisions with the walls focus a particle into the cylinder passing through the openings connecting neighboring compartments. Spending all time in the cylinder, the particle is unaware of varying tube geometry. Therefore, the mobility approaches μ_0 as $F \rightarrow \pm\infty$.^{9,10}

When the constraint geometry changes abruptly, the picture of the particle motion is very different. The reason is that in such systems mobility $\mu(F)$ is a monotonic function of F . For the tube shown in Fig. 1, the mobility monotonically increases with F as shown in Fig. 2. In this case $\mu(F) \rightarrow \mu_0$, as $F \rightarrow +\infty$, since focusing collisions with the walls keep the particle in the narrow cylinder connecting the openings (shown in Fig. 1 by dashed lines). When $F \rightarrow -\infty$, the pattern of the particle motion is the same as that in a cylindrical tube of radius R separated into identical compartments by infinitely thin periodic partitions with circular openings of radius a in their centers studied in Refs. 10(a, b), 11, and 12. In such a tube the particle can be either in the cylinder connecting the openings or in thin layers of thickness $|k_B T/F|$ near the vertical walls. The particle can move in the force direction only when it is in the cylinder. The probability of finding the particle in the cylinder is given by the ratio $a^2/R^2 = \nu^2$, since the marginal distribution of the particle over the tube cross section is uniform and given by $1/(\pi R^2)$, independent of F . As a result, the particle mobility in such a tube approaches its limiting value $\mu_0 \nu^2$, as $F \rightarrow \pm\infty$. This is just the particle mobility in the tube shown in Fig. 1, as $F \rightarrow -\infty$ (Fig. 2).

When the force switches between the two values, $|F|$ and $-|F|$, the displacements in the adiabatic regime are $\mu(\pm|F|)|F|\tau/2$, respectively, and the effective drift velocity is $v_{ad}(|F|) = [\mu(|F|) - \mu(-|F|)]|F|/2$. In the cases of a periodic energy potential and smoothly varying tube geometry, the difference $\mu(|F|) - \mu(-|F|)$ is non-monotonic in $|F|$: it

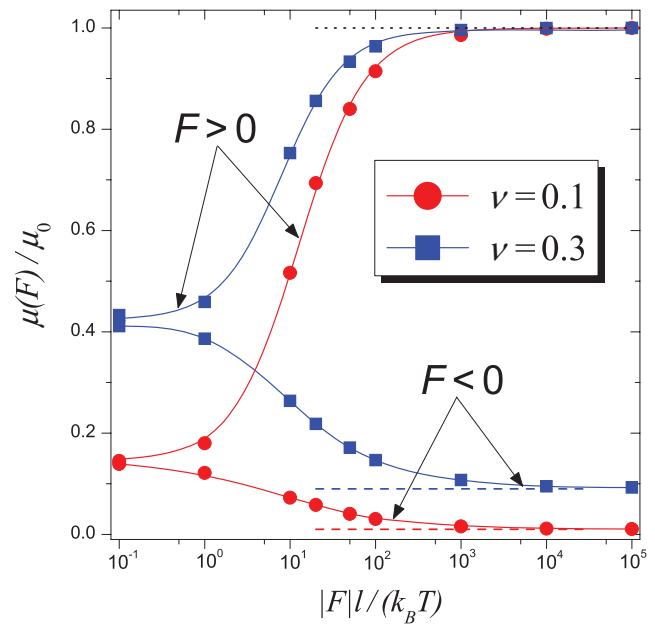


FIG. 2. Particle mobilities scaled by μ_0 as functions of the driving force for the tube shown in Fig. 1 with $\nu = 0.1$ and $\nu = 0.3$, $\nu = a/R$, and $l = R$. Symbols are $\mu(F)/\mu_0$ obtained from Brownian dynamics simulations, and the solid lines are smooth fits of the simulation results. The dashed lines show the large- F asymptotic values of the mobilities scaled by μ_0 . The simulation results were obtained by averaging over 10^5 trajectories. The time step in the simulations varied from $2 \times 10^{-6} R^2/D_0$ to $1.25 \times 10^{-7} R^2/D_0$ depending on the values of the force and the radii ratio ν . When the increment of the trajectory crossed the tube wall, only its component parallel to the wall was accepted, while the component normal to the wall was ignored.

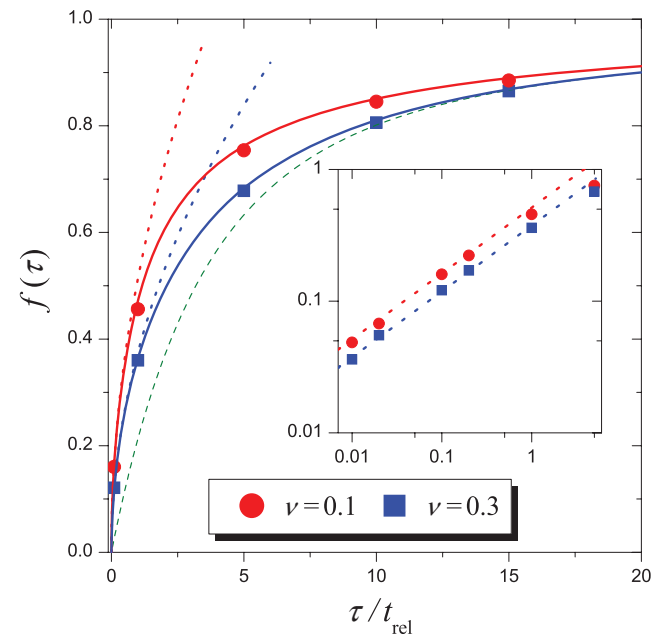


FIG. 3. Comparison of analytical and numerical results. Solid curves represent the plots of $f(\tau)$ given in Eq. (11) at $\nu = 0.1$ (upper curve) and $\nu = 0.3$ (lower curve). The dotted curves represent corresponding small- τ asymptotic behaviors, Eq. (7). The dashed curve represents the plot of $f(\tau)$ in Eq. (8). Symbols are the results obtained from 3D Brownian dynamics simulations. The insert shows $f(\tau)$ at small τ/t_{rel} , where the expressions in Eqs. (7) and (11) are indistinguishable. The simulation results were obtained by averaging over 2.5×10^4 trajectories. The time step in the simulations was $8 \times 10^{-8} R^2/D_0$ for both values of the radii ratio ν . When the increment of the trajectory crossed the tube wall, only its component parallel to the wall was accepted, while the component normal to the wall was ignored.

vanishes as $|F| \rightarrow 0$ and ∞ , having a maximum in-between. As a consequence, $v_{ad}(|F|)$ is also non-monotonic in $|F|$: the velocity first increases with $|F|$, reaches a maximum and then decreases. When the tube geometry changes abruptly, the difference in the mobilities monotonically increases with $|F|$, tending to its maximum value $\Delta\mu_{\max} = \mu(\infty) - \mu(-\infty) = \mu_0(1 - v^2)$, as $|F| \rightarrow \infty$. As a result, $v_{ad}(|F|)$ takes the form

$$v_{ad}(|F|) = \frac{\Delta\mu_{\max}}{2}|F| = \frac{\mu_0(1 - v^2)}{2}|F|, \quad |F| \rightarrow \infty, \quad (1)$$

which shows that $v_{ad}(|F|)$ becomes unboundedly large as $|F| \rightarrow \infty$. Considered as a function of v , $v_{ad}(|F|)$ increases monotonically as v decreases, approaching its maximum value $\mu_0|F|/2$ as $v \rightarrow 0$. This is easy to understand since during positive half-period of the force, when the particle moves forward, its mobility is μ_0 , while during the negative half-period, the particle practically does not move.

Now we proceed to the dependence of the effective drift velocity on the force period. We assume that $|F|$ is large enough, so that as $\tau \rightarrow \infty$, $v(|F|, \tau)$ tends to $v_{ad}(|F|)$ given in Eq. (1). Let us suppose that the force period significantly exceeds the times that characterize the relaxation of the reduced probability density of the particle, after the external force changes its direction. Then most of the positive half-period of the force, the particle is localized in the cylinder connecting the openings. When the force changes its direction from positive to negative, the distribution relaxes to a new steady state, which is identical to that in the cylindrical tube with infinitely thin periodic partitions. This distribution relaxes again to the one in which the particle is localized in the cylinder connecting the openings, when the force changes its direction back from negative to positive.

The two relaxation processes are characterized by the relaxation times, $t_{rel}^{(+ \rightarrow -)}$ and $t_{rel}^{(- \rightarrow +)}$, respectively. It is natural to assume that time $t_{rel}^{(- \rightarrow +)}$ is of the order of $l/(\mu_0|F|)$. (Our simulations support this assumption.) The second relaxation time can be obtained using the results of Ref. 13. This time is independent of $|F|$ and given by

$$t_{rel}^{(+ \rightarrow -)} = \frac{a^2}{4D(1 - v^2)}(v^2 - 1 - \ln v^2). \quad (2)$$

Thus, there are two characteristic time scales, one of which is independent of $|F|$, $t_{rel}^{(+ \rightarrow -)}$ in Eq. (2), whereas the second is inversely proportional to $|F|$, $t_{rel}^{(- \rightarrow +)} \propto 1/|F|$, and vanishes as $|F| \rightarrow \infty$.

We will assume that $|F|$ is large enough, so that $\tau \gg t_{rel}^{(- \rightarrow +)}$, and the particle displacement during the positive half-period of the force, $\Delta_+ = \mu_0|F|\tau/2$, is much larger than l , $\mu_0|F|\tau \gg l$. During the negative half-period of the force, when the particle can be either in the cylinder connecting the openings or in the thin layers near the vertical walls, its displacement is given by $\Delta_- = \mu_0|F| \int_0^{\tau/2} P_{cyl}(t)dt$, where $P_{cyl}(t)$ is the probability of finding the particle in the cylinder at time t , $P_{cyl}(0) = 1$. We use the two displacements to find

$$v(|F|, \tau),$$

$$v(|F|, \tau) = \frac{\Delta_+ - \Delta_-}{\tau} = \frac{\mu_0|F|}{2} \left(1 - \frac{2}{\tau} \int_0^{\tau/2} P_{cyl}(t)dt \right). \quad (3)$$

It is convenient to write $P_{cyl}(t)$ in terms of the relaxation function $R(t)$, that describes the relaxation of $P_{cyl}(t)$ from unity at $t = 0$ to the equilibrium probability of finding the particle in the cylinder, $P_{cyl}^{eq} = v^2$, as $t \rightarrow \infty$. Using the relation $P_{cyl}(t) = P_{cyl}^{eq} + (1 - P_{cyl}^{eq})R(t)$, we can write Eq. (3) as

$$v(|F|, \tau) = v_{ad}(|F|)f(\tau), \quad f(\tau) = 1 - (2/\tau) \int_0^{\tau/2} R(t)dt, \quad (4)$$

where $v_{ad}(|F|)$ is given in Eq. (1).

The asymptotic behaviors of $f(\tau)$ in the limiting cases of $\tau \rightarrow \infty$ and 0 can be readily found. As $\tau \rightarrow \infty$, $f(\tau)$ in Eq. (4), takes the form

$$f(\tau) \approx 1 - 2t_{rel}/\tau, \quad \tau \rightarrow \infty, \quad (5)$$

where $t_{rel} = t_{rel}^{(+ \rightarrow -)}$ is the relaxation time defined by (hereafter we omit the superscript)

$$t_{rel} = \int_0^\infty R(t)dt = \int_0^\infty [P_{cyl}(t) - P_{cyl}^{eq}]dt / (1 - P_{cyl}^{eq}), \quad (6)$$

which is given in Eq. (2). To find the small- τ asymptotic behavior of $f(\tau)$ we use the relation $R(t) = [P_{cyl}(t) - P_{cyl}^{eq}]/[1 - P_{cyl}^{eq}]$ and the short-time asymptotic behavior of $P_{cyl}(t)$, $P_{cyl}(t) \approx 1 - (2/a)\sqrt{Dt/\pi}$, $t \rightarrow 0$, which is easy to obtain. This leads to $R(t) \approx 1 - (2/a)\sqrt{Dt/\pi}/(1 - v^2)$, $t \rightarrow 0$. Substituting this into Eq. (4), we find

$$f(\tau) \approx 2\sqrt{2D\tau/\pi}/[3a(1 - v^2)], \quad \tau \rightarrow 0. \quad (7)$$

Note that the small- τ asymptotic behavior of the effective drift velocity, $v(|F|, \tau) \propto \sqrt{\tau}$, is quite different from the small- τ asymptotic behavior $v(|F|, \tau) \propto \tau^4$, obtained for the case of smoothly varying energy potential.¹⁴

Using t_{rel} we can obtain a simple formula for $f(\tau)$ by approximately modeling transitions between mobile (m) and immobile (im) states of the particle (i.e., in the cylinder and near the walls, respectively) as a two-state Markov process $m \xrightleftharpoons[k_{im}]{k_m} im$, where $k_m = (1 - v^2)/t_{rel}$ and $k_{im} = v^2/t_{rel}$ are the rate constants. This leads to a single-exponential approximation of the relaxation function, $R_{exp}(t) = \exp(-t/t_{rel})$. Substituting $R_{exp}(t)$ into the expression for $f(\tau)$ in Eq. (4) and carrying out the integration, we arrive at

$$f(\tau) \approx f_{exp}(\tau) = 1 - (2t_{rel}/\tau)(1 - e^{-\tau/(2t_{rel})}). \quad (8)$$

This simple expression describes a monotonic increase of $f(\tau)$ from zero to unity as τ increases from zero to infinity, and reduces to the exact result in Eq. (5) as $\tau \rightarrow \infty$.

Finally, we obtain a rigorous solution for $f(\tau)$ over the entire range of τ using the eigenfunction expansion of the

propagator,

$$g(r, t|r_0) = \frac{1}{\pi R^2} \left[1 + \sum_{n=1}^{\infty} \frac{J_0(\lambda_n r) J_0(\lambda_n r_0)}{J_0^2(\lambda_n R)} e^{-\lambda_n^2 D t} \right], \quad (9)$$

where $J_k(z)$ is the Bessel function of the first kind of order k , and λ_n is the n th positive root of the equation $J_1(\lambda_n R) = 0$, $n = 1, 2, \dots$. First, we find the probability $P_{cyl}(t)$

$$P_{cyl}(t) = P_{cyl}^{eq} + \frac{4}{R^2} \sum_{n=1}^{\infty} \frac{J_1^2(\lambda_n a)}{\lambda_n^4 J_0^2(\lambda_n R)} e^{-\lambda_n^2 D t}, \quad (10)$$

and the relaxation function, $R(t) = [P_{cyl}(t) - v^2]/(1 - v^2)$, which we substitute into Eq. (4). Carrying out the integration we arrive at

$$f(\tau) = 1 - \frac{8}{D\tau(R^2 - a^2)} \sum_{n=1}^{\infty} \frac{J_1^2(\lambda_n a)}{\lambda_n^4 J_0^2(\lambda_n R)} (1 - e^{-\lambda_n^2 D \tau/2}). \quad (11)$$

This is the exact solution for $f(\tau)$ on condition that $\mu_0|F|\tau \gg l$, so that the inequality $\tau \gg t_{rel}^{(- \rightarrow +)}$ is fulfilled. Neglecting the exponential terms, we obtain the expression for $f(\tau)$ in Eq. (5) with t_{rel} given by

$$t_{rel} = \frac{4}{(R^2 - a^2)D} \sum_{n=1}^{\infty} \frac{J_1^2(\lambda_n a)}{\lambda_n^4 J_0^2(\lambda_n R)}, \quad (12)$$

which is an alternative representation of the relaxation time. The two expressions for t_{rel} , Eqs. (2) and (12), are exact results obtained by means of different formalisms. The eigenfunction expansion of the propagator leads to the result in Eq. (12), whereas the result in Eq. (2) can be derived using the Laplace transform of the propagator.¹³

Our analytical results are compared with those obtained from 3D Brownian dynamics simulations in Fig. 3, where we show the plots of $f(\tau)$ given in Eqs. (8) and (11), as well as the small- τ asymptotic behavior in Eq. (7) as functions of the ratio τ/t_{rel} . The expression in Eq. (8) is a universal function of τ/t_{rel} in the sense that it is independent of v , whereas the expressions in Eqs. (7) and (11) depend on v . Symbols in Fig. 3 show the values of $f(\tau)$ found from Brownian dynamics simulations at $|F| = 10^5 k_B T/l$, for tubes with $l/R = 1$, and $v = 0.1, 0.3$. The force $|F| = 10^5 k_B T/l$ is large in the sense that the mobility difference is very close to its asymptotic value $\Delta\mu_{\max} = \mu_0(1 - v^2)$ in both tubes (Fig. 2). Therefore, we obtained $f(\tau)$ as the ratio of the effective drift velocity found from simulations to $v_{ad}(|F|)$ given in Eq. (1). The comparison shows excellent agreement between the theoretical predictions and numerical results for both tubes.

To summarize, our analysis of directed motion of a particle induced by a time-periodic force of amplitude $|F|$ with zero mean, in a periodically tapered tube (Fig. 1) is based on two observations. First, the particle mobility in such a tube monotonically increases with the driving force (Fig. 2). Second, the relaxation time $t_{rel}^{(+ \rightarrow -)} = t_{rel}$ is independent of $|F|$, Eq. (2), whereas the relaxation time $t_{rel}^{(- \rightarrow +)}$ is proportional to $|F|^{-1}$ and becomes vanishingly small as $|F| \rightarrow \infty$. Using these two facts, we derive an analytical solution for the effective drift velocity at large $|F|$ that describes the velocity dependence on the amplitude and period of the force and the geometric parameters of the tube. Our analytical results are corroborated by the results of Brownian dynamics simulations (Fig. 3).

This study was supported by the Russian Foundation for Basic Research (Grant No. 10-03-0093) and the Intramural Research Program of the National Institutes of Health (NIH), Center for Information Technology.

- ¹P. Reimann, *Phys. Rep.* **361**, 57 (2002); P. Hanggi, F. Marchesoni, and F. Nori, *Ann. Phys. (Leipzig)* **14**, 51 (2005); P. Hanggi and F. Marchesoni, *Rev. Mod. Phys.* **81**, 387 (2009).
- ²C. Kettner, P. Reimann, P. Hanggi, and F. Muller, *Phys. Rev. E* **61**, 312 (2000).
- ³C. Marquet, A. Buguin, L. Talini, and P. Silberzan, *Phys. Rev. Lett.* **88**, 168301 (2002).
- ⁴S. Matthias and F. Muller, *Nature (London)* **424**, 53 (2003).
- ⁵B. Q. Ai and L. G. Liu, *Phys. Rev. E* **74**, 051114 (2006); *J. Chem. Phys.* **126**, 204706 (2007); B. Q. Ai, H. Z. Xie, and L. G. Liu, *Phys. Rev. E* **75**, 061126 (2007); B. Q. Ai, *ibid.* **80**, 011113 (2009); *J. Chem. Phys.* **131**, 054111 (2009).
- ⁶G. Schmid, P. S. Burada, P. Talkner, and P. Hanggi, *Adv. Solid State Phys.* **48**, 317 (2009).
- ⁷F. Marchesoni and S. Savel'ev, *Phys. Rev. E* **80**, 011120 (2009).
- ⁸R. L. Stratonovich, *Radiotekh. Elektron. (Moscow)* **3**, 497 (1958); H. Risken, *The Fokker-Planck Equation* (Springer-Verlag, Berlin, 1984).
- ⁹D. Reguera, G. Schmid, P. S. Burada, J. M. Rubi, P. Reimann, and P. Hänggi, *Phys. Rev. Lett.* **96**, 130603 (2006); P. S. Burada, G. Schmid, P. Talkner, P. Hänggi, D. Reguera, and J. M. Rubi, *BioSystems* **93**, 16 (2008); P. S. Burada, P. Hänggi, F. Marchesoni, G. Schmid, and P. Talkner, *ChemPhysChem* **10**, 45 (2009); N. Laachi, M. Kenward, E. Yariv, and K. D. Dorfman, *Europhys. Lett.* **80**, 5009 (2007).
- ¹⁰(a) A. M. Berezhkovskii, L. Dagdug, Yu. A. Makhnovskii, and V. Yu. Zitserman, *J. Chem. Phys.* **132**, 221104 (2010); (b) L. Dagdug, A. M. Berezhkovskii, Yu. A. Makhnovskii, V. Yu. Zitserman, and S. M. Bezrukov, *ibid.* **134**, 101102 (2011); (c) A. M. Berezhkovskii and L. Dagdug, *ibid.* **133**, 134102 (2010).
- ¹¹F. Marchesoni, *J. Chem. Phys.* **132**, 166101 (2010).
- ¹²Yu. A. Makhnovskii, A. M. Berezhkovskii, L. V. Bogachev, and V. Yu. Zitserman, *J. Phys. Chem. B* **115**, 3992 (2011).
- ¹³A. M. Berezhkovskii, *Chem. Phys.* **370**, 253 (2010).
- ¹⁴P. Reimann, in *Lecture Notes in Physics* (Springer-Verlag, Berlin, 2000), Vol. 557, pp. 50–60.